

SUPPLEMENTARY INFORMATION

Development of multi-drug loaded PEGylated nanodiamonds to inhibit tumor growth and metastasis in genetically engineered mouse models of pancreatic cancer

Vijay S. Madamsetty,¹ Krishnendu Pal,¹ Sandeep Keshavan,³ Thomas R. Caulfield,⁴ Shamit Kumar Dutta,¹ Enfeng Wang,¹ Bengt Fadeel³, and Debabrata Mukhopadhyay^{1,2,*}

¹Department of Biochemistry and Molecular Biology, and ²Department of Physiology and Biomedical Engineering, Mayo Clinic College of Medicine and Science, Jacksonville, FL 32224, United States;

³Division of Molecular Toxicology, Institute of Environmental Medicine, Karolinska Institutet, 171 77

Stockholm, Sweden; ⁴Department of Neuroscience, Mayo Clinic College of Medicine and Science, Jacksonville, FL 32224, United States.

*Corresponding author: Prof. Debabrata Mukhopadhyay, Mayo Clinic College of Medicine and Science, 4500 San Pablo Road, Jacksonville, FL 32224, United States, E-mail: mukhopadhyay.debabrata@mayo.edu;

Molecular modeling

Building the Models.

Using our established computational techniques and other published methods we modeled the ND complexes¹⁻³. A nanodiamond system was built as described in the main text. Further details are reported here. Hence, a disordered system builder requires a Materials Science Suite, which we used Desmond system builder to set solvent, PBC, and FF⁴⁻⁶. The first key here is assigning OPLS3 FF, which automatically assigns UFF parameters for ND atoms. The second key here is setting the position

restraints: 1. Desmond system builder to set PBC (orthorhombic with minimal volume) and OPLS3 FF⁷ were used for design. 2. Load the system builder output from Desmond minimization panel. 3. Run minimization. 4. Once minimization is done, repeat 2-3 with molecular dynamics panel to run equilibration MD (NVT-310K) simulations and final production run simulations with NPT ensemble.

Simulating the Models

I. Equilibrating Simulations. Using the super-fast version of GPU-Desmond, we performed equilibration for 1.0 ns NVT simulation over the 230,000-atom system in just under 3 hours and the nanodiamond stays intact. We then started longer molecular dynamics simulations (MDS) using NVE/NPT ensembles for >100 ns for equilibration. II. Molecular Dynamics Simulation (NPT production runs). After the system was minimized with relaxed restraints using Steepest Descent and Conjugate Gradient PR, and equilibrated in the solvent with physiological salt conditions, as described in the literature^{6, 8} and equilibration established, each system was allowed to run an additional MD production length of >10 nanoseconds. The primary purpose of MD for this study was conformational stability, structure refinement, and interaction calculations at the drug-ND interface.

II. Molecular dynamics simulations protocol followed. OPLS3 (Desmond setup) and Nanoscale Molecular Dynamics 2 (NAMD2)^{9, 10} were used for studying the dynamics behavior of these systems. All simulations included solute ions and water molecules comprising an average complete system size of 2.5×10^5 atoms using SPC water and ions. In all cases, we neutralized with counter-ions, and then created a solvent with 125 mM Na⁺ Cl⁻ to recreate physiological strength. SPC water molecules were added around the protein at a depth of 15-18 Å from the edge of the molecule depending upon the side. Our protocol has been previously described in the literature⁸. Simulations were carried out using the particle mesh Ewald technique with repeating boundary conditions with a 9 Å non-bonded cut-off, using SHAKE with a 2-fs time step. Pre-equilibration was started with three stages of minimization with 10,000 steps of SD, PRCG, relaxing restraints, then followed by 1000 ps of heating under MD, with the atomic positions of nucleic and protein fixed. Then, two cycles of minimization (5000 steps

each) and heating (1000 ps) were carried out with soft restraints of 10 and 5 kcal/(mol·Å²) applied to all backbone atoms and metals. Next, 5000-steps of minimization were performed with solute restraints reduced to 1 kcal/(mol·Å²). Following that, 400 ps of MDS were completed using relaxing restraints (1 kcal/(mol·Å²)) until all atoms are unrestrained, while the system was slowly heated from 1 to 310 K using velocity rescaling upon reaching the desired 310K during this equilibration phase. Additionally, NPT production runs with velocity rescaling for >10 ns were completed with constant pressure boundary conditions (relaxation time of 1.0 ps). A constant temperature of 310 K was maintained using the Berendsen weak-coupling algorithm with a time constant of 1.0 ps. SHAKE constraints were applied to all hydrogens to eliminate X-H vibrations, which yielded a longer simulation time step (2 fs). Our methods for equilibration and production run protocols are in the literature^{5 6 11}. Translational and rotational center-of-mass motions were initially removed. Periodically, simulations were interrupted to have the center-of-mass removed again by subtraction of velocities to account for the “flying ice-cube” effect¹². Following the simulation, the individual frames were superposed back to the origin, to remove rotation and translation effects.

Supplementary Figures

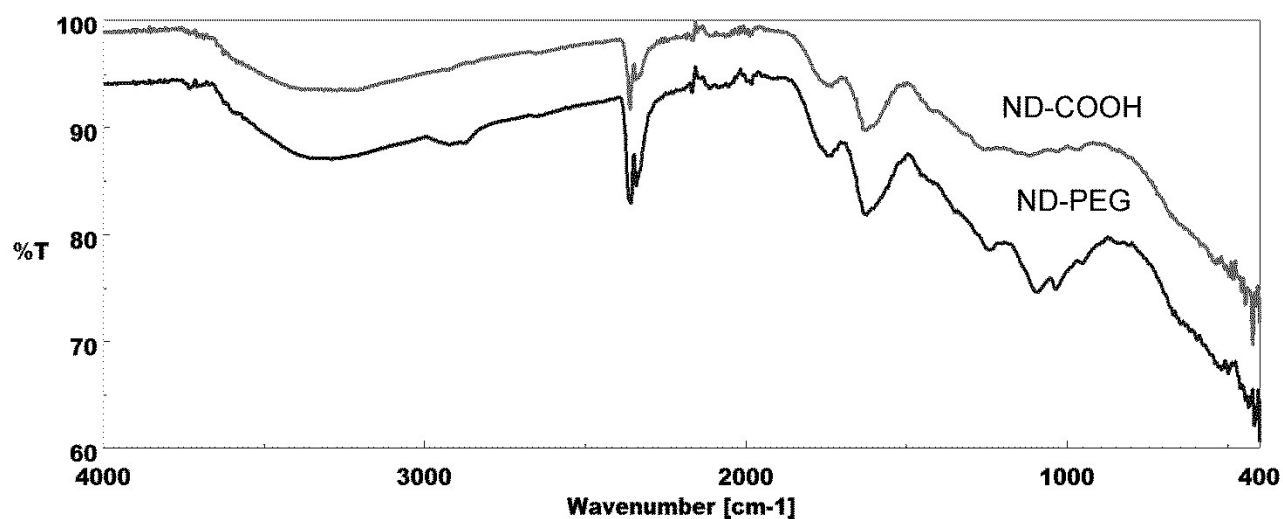


Figure S1. Confirmation of PEGylation through FTIR. FTIR analysis of ND-COOH and ND-PEG

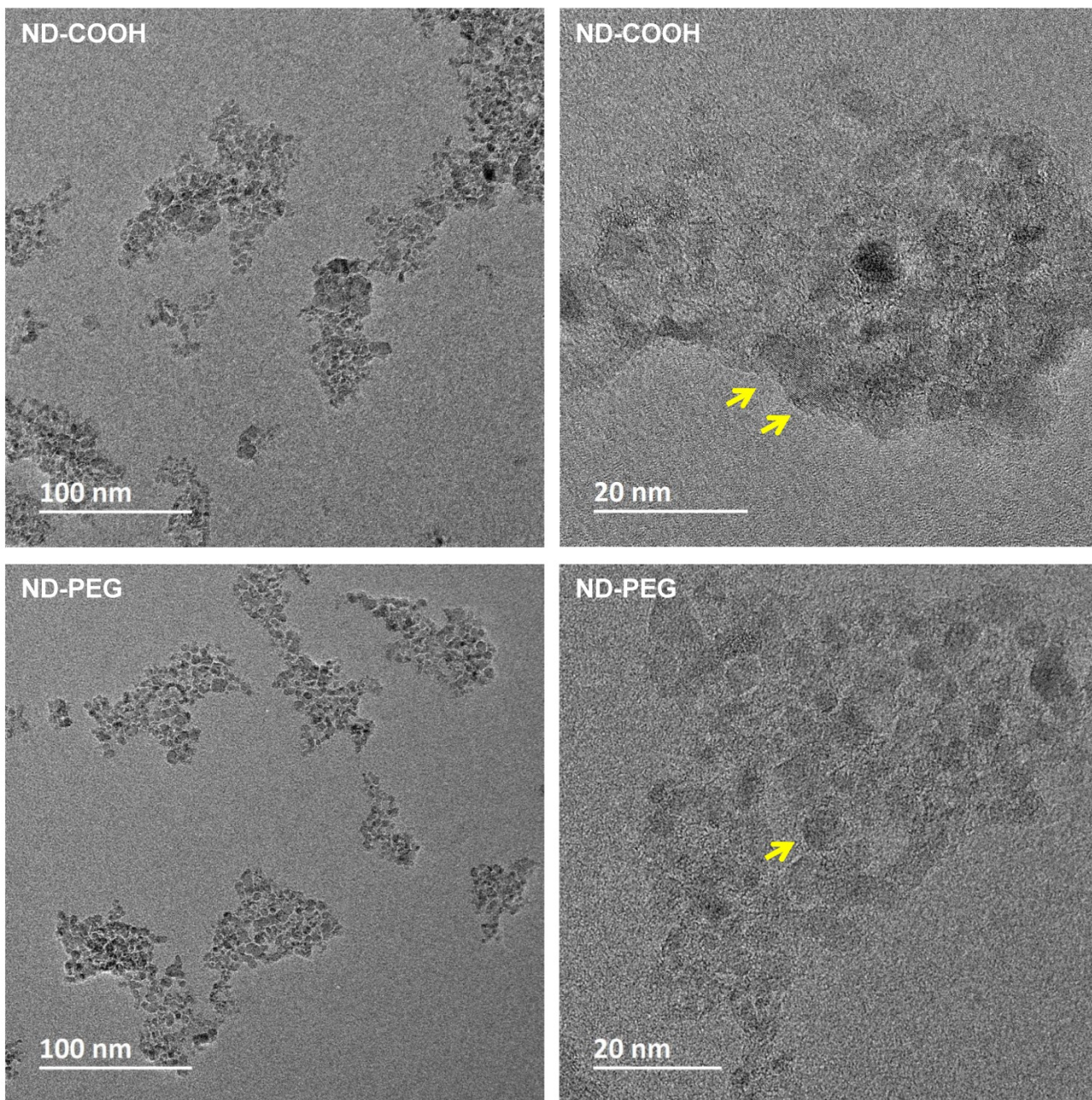


Figure S2. HR-TEM imaging of NDs without drugs. The arrows are pointing at the (111) diamond lattice lines, evidenced both in ND-COOH (upper panels) and PEGylated NDs (lower panels).

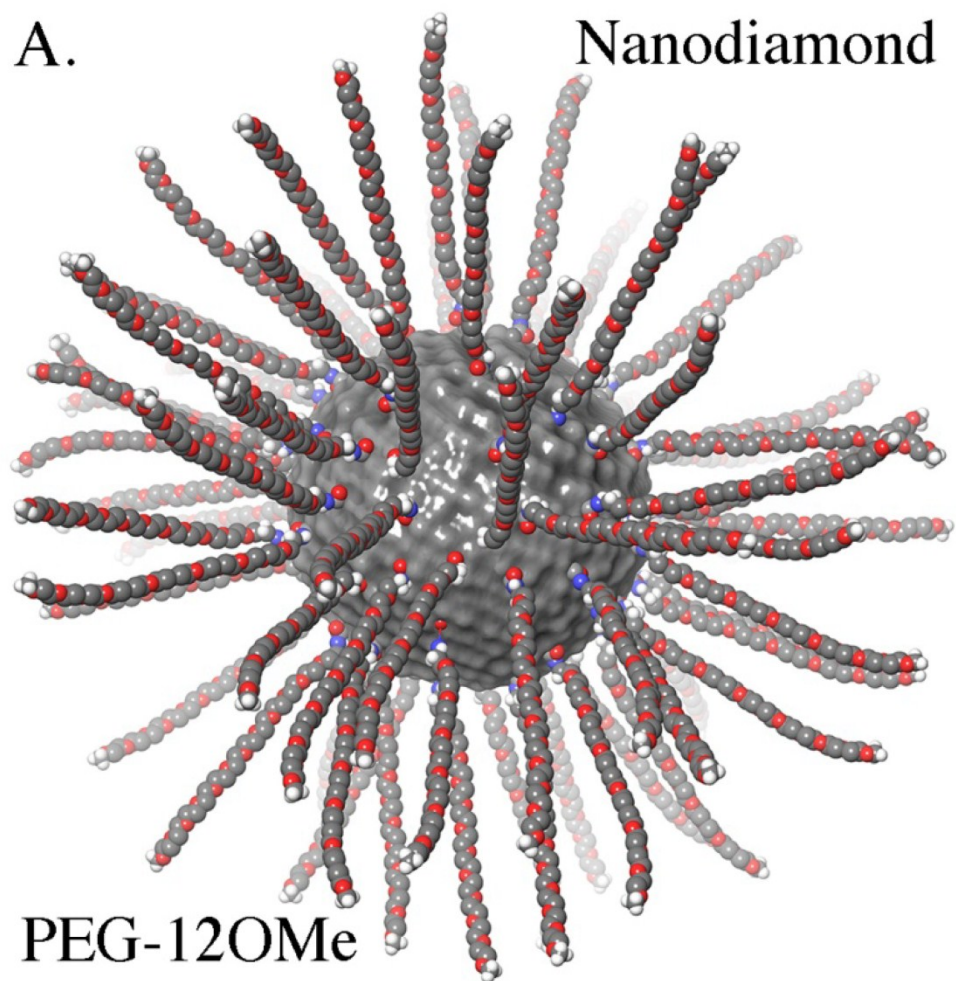


Figure S3. Molecular modeling studies of PEGylated nanodiamond. (A) Computational modeling for PEGylated ND.

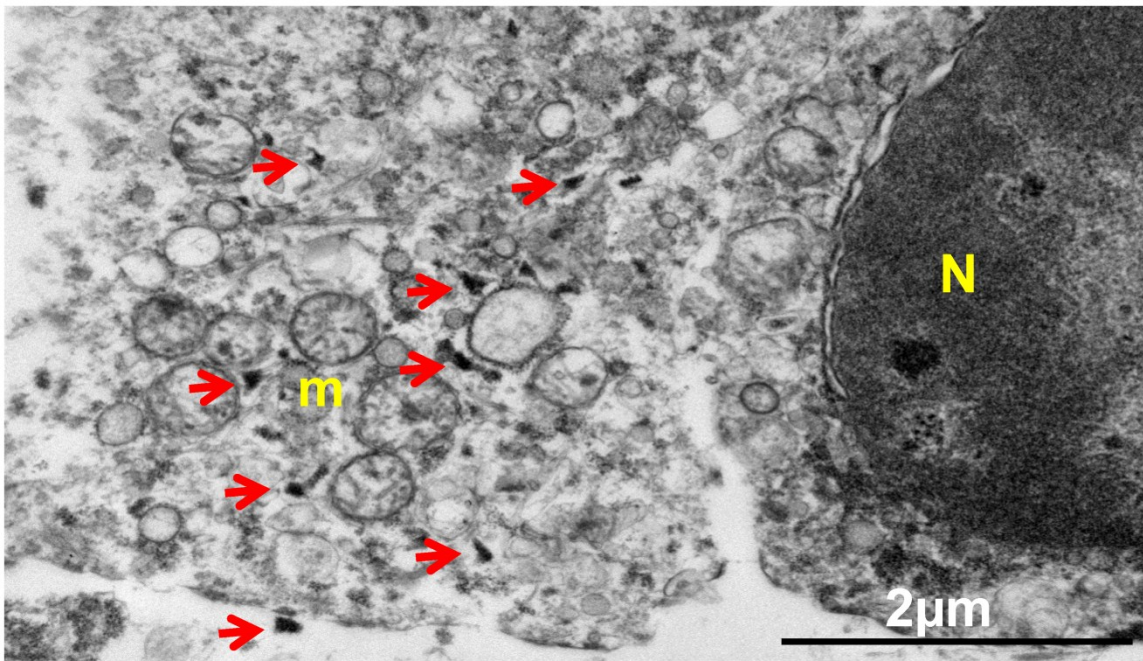


Figure S4: TEM images are showing the presence of NDs in the tumor sections indicated with arrows (blue color). Scale bar= 2 μ m

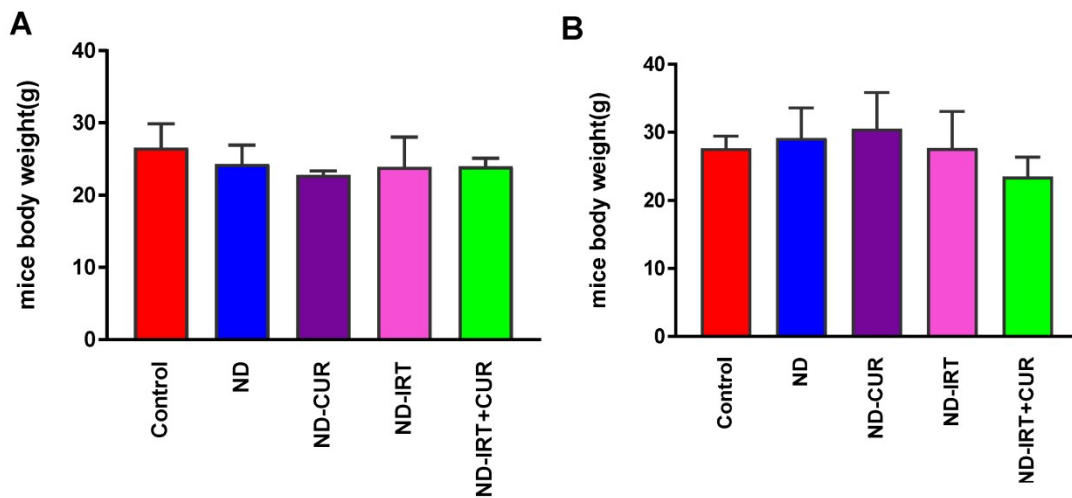


Figure S5. No abnormalities concerning body weight from *in vivo* studies. (A) Endpoint mice body weight in Ca5Cre adenovirus implanted orthotopically in KPC (P53 knockout) mice after 2x/wk treatment for four weeks with vehicle control, ND, ND-IRT (5 mg kg⁻¹ IRT equivalent), CUR (15 mg kg⁻¹ CUR equivalent) and ND-IRT+CUR (5 mg kg⁻¹ IRT equivalent + 15 mg kg⁻¹ CUR equivalent). (B)

The corresponding data for KPC-with mutant p53 mice with tumors initiated by orthotopically implanting Ca5Cre adenovirus. The data in (A) and (B) are shown as mean values \pm S.D. (n=5).

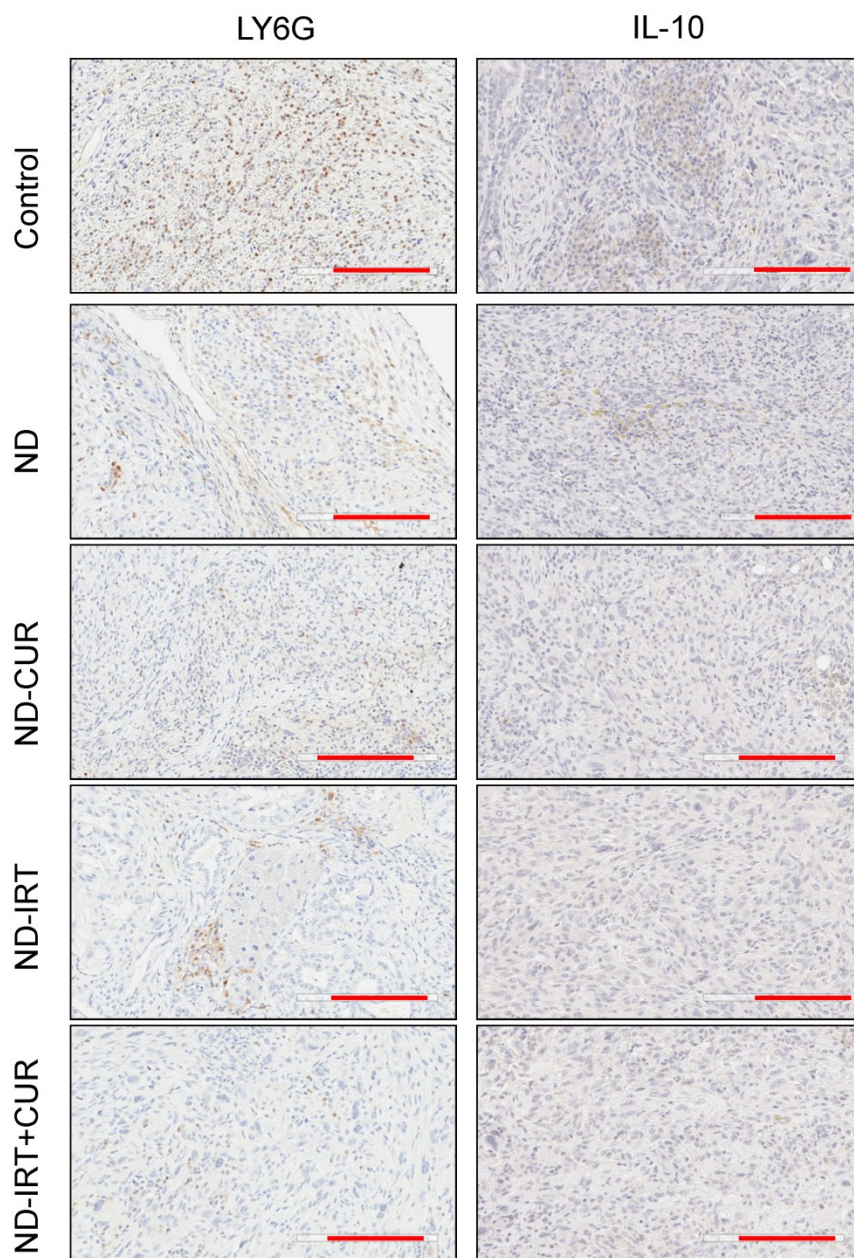


Figure S6. Immunohistochemistry (IHC) of tumor sections for LY6G and IL-10 staining. After 2x/wk treatment for 4 weeks with vehicle control, ND, ND-IRT (5 mg kg⁻¹ IRT equivalent), CUR (15

mg kg⁻¹ CUR equivalent) and ND-IRT+CUR (5 mg kg⁻¹ IRT equivalent +15 mg kg⁻¹ CUR equivalent) tumor sections were stained for LY6G and IL-10 expression.

Supplementary Movies



Movie S1.mpeg

Movie S1. Animation for the drug-bound (captured) nanodiamond complex.

Supplementary Table S1. Hydrodynamic diameters of NDs with/without drugs.

Sample	Water		DMEM + 10% FBS		RPMI + 10% FBS	
	size (nm)	PDI	size (nm)	PDI	size (nm)	PDI
ND	11 ± 5	0.4 ± 0.01	105 ± 15	0.32 ± 0.01	88 ± 16	0.33 ± 0.01
ND-IRT	18 ± 3	0.2 ± 0.01	123 ± 18	0.24 ± 0.01	96 ± 10	0.19 ± 0.01
ND-CUR	19 ± 2	0.2 ± 0.01	68 ± 10	0.22 ± 0.01	112 ± 4	0.34 ± 0.01
ND-IRT+CUR	19.2 ± 2	0.21 ± 0.01	95 ± 17	0.321 ± 0.01	128 ± 8	0.24 ± 0.01

Supplementary Table S2: Combination index (CI) Values for curcumin (Cur) and Irinotecan (IRT) used in our present study

	CI values for 80% inhibition	CI values for 30 % inhibition
AsPC1	0.87	0.53
PANC-1	0.75	0.5

References

1. W. Humphrey, A. Dalke and K. Schulten, *J Mol Graph*, 1996, **14**, 33-38, 27-38.
2. Schrödinger, *Journal*, 2013.
3. R. A. Laskowski, M. W. MacArthur, D. S. Moss and J. M. Thornton, *J Appl Cryst*, 1993, **26**, 283-291.

4. D. Shivakumar, J. Williams, Y. Wu, W. Damm, J. Shelley and W. Sherman, *J Chem Theory Comput*, 2010, **6**, 1509-1519.
5. T. Caulfield and B. Devkota, *Proteins*, 2012, **80**, 2489-2500.
6. T. R. Caulfield, B. Devkota and G. C. Rollins, *J Biophys*, 2011, **2011**, 219515.
7. E. Harder, W. Damm, J. Maple, C. Wu, M. Reboul, J. Y. Xiang, L. Wang, D. Lupyan, M. K. Dahlgren, J. L. Knight, J. W. Kaus, D. S. Cerutti, G. Krilov, W. L. Jorgensen, R. Abel and R. A. Friesner, *J Chem Theory Comput*, 2016, **12**, 281-296.
8. T. R. Caulfield, *Journal of molecular graphics & modelling*, 2011, **29**, 1006-1014.
9. D. A. Case, T. E. Cheatham III, T. Darden, H. Gohlke, R. Luo, K. M. Merz Jr, A. Onufriev, C. Simmerling, B. Wang and R. Woods, *Journal of Chemical Chemistry*, 2005, **26**, 1668-1688.
10. J. C. Phillips, R. Braun, W. Wang, J. Gumbart, E. Tajkhorshid, E. Villa, C. Chipot, R. Skeel, L. Kale and K. Schulten, *Journal of Computational Chemistry*, 2005, **26**.
11. K. Reblova, F. Lankas, F. Razga, M. V. Krasovska, J. Koca and J. Sponer, *Biopolymers*, 2006, **82**, 504-520.
12. T. E. Cheatham, III and M. A. Young, *Biopolymers*, 2001, **56**, 232-256.